American Journal of Applied Sciences 4 (9): 718-724, 2007
ISSN 1546-9239

Studies on the Influence of Various Blade Outlet Angles in a Centrifugal Pump when Handling Viscous Fluids

M. H. Shojaee Fard and F.A. Boyaghchi
Department of Mechanical Engineering, University of Science and Technology of Iran, Tehran, Iran

Abstract: In this study the centrifugal pump performances with different blade outlet angles are tested when handling water and viscous oils as Newtonian fluids. Also, this study shows a numerical simulation of the three-dimensional fluid flows inside the centrifugal pump with different blade outlet angles. For these numerical simulations the SIMPLEC algorithm is used for solving governing equations of incompressible viscous/turbulent flows through the pump at different operating conditions. The k-ε turbulence model is adopted to describe the turbulent flow process. These simulations have been made with a steady calculation using the multiple reference frames (MRF) technique to take into account the impeller- volute interaction. Numerical results are compared with the experimental characteristic curve for each viscous fluid. The results show that when the outlet angle increases, the centrifugal pump performance handling viscous fluids improves. This improvement is due to decrease of wake at the exit of impeller. Also the results show that the well-known jet/wake flow model is not found in the impeller simulations.

Keywords: Centrifugal pump, performance, newtonian fluids, viscous fluid flow, blade outlet angle, 3D numerical simulation, experimental test

INTRODUCTION

When a fluid of high viscosity -such as heavy oil- is pumped by a centrifugal pump the performance is impaired in comparison to service with water due to increased losses. Viscosity is defined as resistor to pouring with higher viscosity fluids affecting centrifugal pump performance by increasing the power, reducing the flow rate, head and efficiency, making trouble for mechanical seals and causing more load on bearings.

Many researches, such as Stepanoff[1], Telow[2], Ippen[3] and Itaya and Nishikawa[4], have tested the performance of the centrifugal oil pumps as a function of the viscosity of the viscous oil without knowing the phenomena of viscous fluid flow within the pump. They have proposed some correction factors when pump handles the viscous fluid for determining the performance. These typical results have provided great insights into the effects of the oil viscosity on the performance of centrifugal oil pumps, which have been applied in the important guidelines used today for the design of these pumps. However, these experimental results are based on the oil pump products available in the 1920s and 1950s. On the other hand, some researches, such as Stoffel[5], Li[6] and Li and Hu[7], conducted experiments using commercial centrifugal oil pumps.

Within the last few years, several computer codes for analyzing the effects of viscosity and boundary layers on turbo machinery performance have been published. The codes use different numerical schemes, boundary conditions and turbulence models for predicting the viscosity effects, impeller tip leakage and secondary flow through blade row. By using this code, Denton[8] simulated the viscous effects in the passage of blades by using of a distributed body force. Miner[9,10] has done several researches on two dimensional flow analysis and turbulence measurements of a centrifugal pump.

Croba and Kueny[11], simulated the 2D, unsteady water flow in centrifugal pump by using the CFD code. Denus and Gode[12], studied a mixed - flow pump impeller when handling low viscous fluid flow by using the CFD analysis. However, due to the difficulties of the task, most of studies have done heavy simplifications of the problem either in the geometry or in the flow characteristics. Research slowly trends towards more complete simulations. Blanco[13,14] simulated the fluid flow in the centrifugal pump for investigating the pressure fluctuates in the volute by using the CFD code.

Investigations show that the geometry of impeller affects the performance of the centrifugal pump when handling viscous fluids. Varley[15] investigated the effects of impeller design and surface roughness on performance of centrifugal pumps. Wengung[16] studied the flows of viscous oil in a centrifugal pump impeller with large discharge and small wrapping angles of blades at different working conditions. Then he[17] studied the influence of the number of impeller blades on the performance of centrifugal oil pumps. Results

Corresponding Author: M. H. Shojaee Fard, Department of Mechanical Engineering, University of Science and Technology of Iran, Tehran, Iran

show the optimum number of blades for various viscous fluids.

Shojaee Fard and Ehghaghi[18] studied the performance of the centrifugal pump experimentally for different geometries of impeller in order to optimizing the centrifugal pump when handling the viscous oil and simulated the fluid flow in a passage of impeller by use of a CFD code.

One of the most important characters, which can effect on the centrifugal pump performance when handling viscous fluids, is the blade outlet angle. This character can weaken or strengthen the wake at the exit of impeller.

In this study the blade outlet angles are studied experimentally and numerically to show their effects on performance of centrifugal pump when handling viscous fluids.

Experimental facility

Test rig: A special centrifugal pump test rig, shown in Fig. 1, is used to test the pump performance and to measure the flow within the pump impeller when the pump is pumping viscous oil and water. The pump tested is driven by a three - phase AC electric motor, whose rated power is 5.5 KW and speed is 1450 rev/min.

Performance test method: The pump suction pressure and discharge pressure are measured by pressure gages. The capacities of the pump are measured by a turbine or nuzzle flow meter. Torque meter measures the shaft torque and speed of the pump. By means of a rotary viscosity meter the viscosity of oil can be given. The density of oil is checked using a floating glass tube density meter.

Impeller geometries: The base centrifugal pump is a 65-200 single axial suction and vane less volute casing equipped with an impeller of 209 mm in outside diameter and 6 backwards curved blades. The blade outlet and wrapping angles of the impeller are 27.5° and 140°. When the pump is run at 1450 rev/min the Best Efficiency Point (BEP) corresponds to 50 m^3/h flow rate and 14 m height. The shroud of the impeller made of metal is machined. The roughness of the impeller and volute is 100 μm. The Fig. 2 and 3 show the impeller configuration and the components of pump respectively.

For investigating the influence of blade outlet angles, two impellers with blade outlet angles of 22.5° and 32.5° are manufactured and simulated. Figure 4 and 5 show the impellers with various blade outlet angles.

Working fluid: Working fluids are the special transparent viscous oil refined from crude oils and tap water, respectively. They are Newtonian fluids verified by using the rotary viscosity meter. The density and kinematic viscosity of the oils are 875 kg/m^3 and

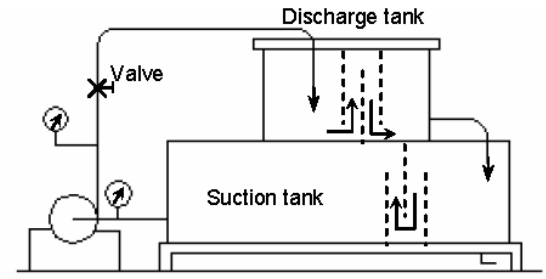

Fig. 1: Centrifugal pump test rig

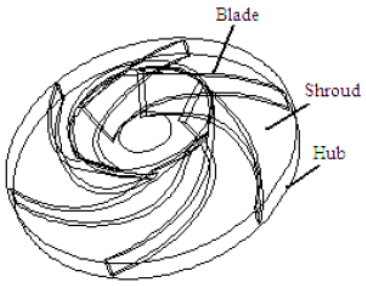

Fig. 2: Impeller configuration with blade outlet angle of 27.5°

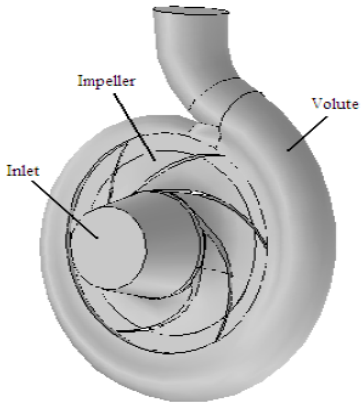

Fig. 3: Components of pump

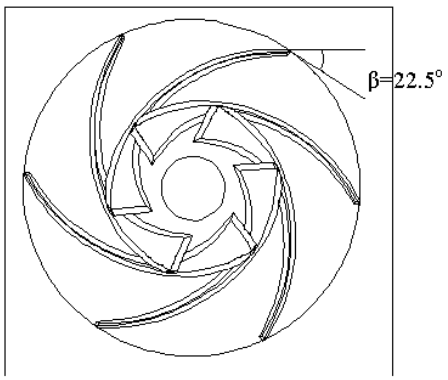

Fig. 4: Impeller with blade outlet angle of 22.5°

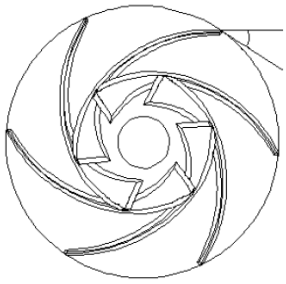

Fig. 5: Impeller with blade outlet angle of 32.5°

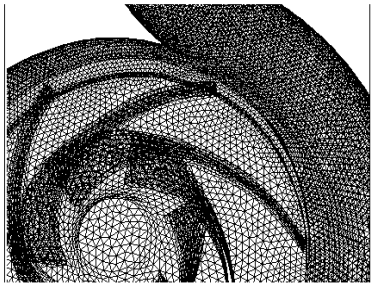

Fig. 6: Sketch of the pump grid

43×10^{-6} m^2/s and 878 kg/m^3 and 62×10^{-6} m^2/s , respectively, at 20°C.The density and the kinematic viscosity of the tap water are 1000 kg/m^3 and 1×10^{-6} m^2/s, respectively, at 20°C. First, the centrifugal pump performance pump performance and flow fields in the impeller were measured using the tap water as a working fluid. Then the performance and flow fields were measured again using the viscous oils as a working fluid.

Experimental uncertainty: The uncertainties in head, capacity, torque, speed and efficiency are 0.4, 0.5, 0.3, 1 and 1.15%, respectively.

Computational method

Pump, geometry and grid: With the three-dimensional model there is a useful approach for investigation of flow behavior in different parts of pump.

The blade number and shape has great importance. A pump with few backward blades gives less distortion in the flow and it is possible to simulate it with a relatively rough mesh. A large number of blades require a great number of cells to correctly simulate the flow passages. Forward blades, because of the severe stall that is usual in the suction side, needs a fine mesh in this area if we want to capture this phenomenon.

Figure 6 shows the unstructured grid generated and Table 1 shows the number of cells in various impeller geometries. These cells are enough for precise boundary layer simulation and they give correct values

Table 1: The number of cells in various impeller geometries

	Inlet	Impeller	Volute	Outlet pipe
22.5°	19279	60817	117532	109964
27.5°	18562	46449	117179	111412
32.5°	18748	46901	116973	109964

for the pumps performance and allow to analysis the details of the main phenomena involved.

Surface between inlet-impeller and impeller-volute correspond to grid interfaces. The multiple reference frame (MRF) technique allows the relative motion of the impeller grid with respect to the inlet and the volute during steady simulation. Grid faces do not need aligned on both sides.

Mathematical model

Basic equations: Continuity and 3-D incompressible Navier-Stokes equations, including the centrifugal force source in the impeller and steady terms are used in centrifugal pump to analyze the turbulent viscous fluid flow. Turbulence process is simulated with the k-ε model. Although grid size is not adequate to correctly take account of boundary layers on blades, wall functions, based on the logarithmic law, has been used. The pressure - velocity coupling is calculated through the SIMPLEC algorithm. Second order, upwind discretizations have been used for convection terms and central difference schemes for diffusion terms.

The continuity and momentum equations can be written in the rotating coordinate system as follows:

$$\nabla.(\rho U) = 0 \tag{1}$$

and

$$\nabla\cdot(\rho U\otimes U) = \nabla\cdot\left(-P\delta+\mu_{eff}\left(\nabla U+(\nabla U)^T\right)\right)+S_M \tag{2}$$

where vector notation has been used, $\otimes$ is a vector cross- product; U is the velocity; P is the pressure; ρ is the density; δ is the identity matrix; and S_M is the source term.

For flows in a rotating frame of reference that are rotating at the constant rotation speed $\vec{\Omega}$, the effects of the Coriolis are modeled in the code. In this case,

$$S_M = -\rho\left[2\vec{\Omega}\otimes U+\vec{\Omega}\otimes\left(\vec{\Omega}\otimes\vec{r}\right)\right] \tag{3}$$

Where $\vec{r}$ is the location vector.

k-ε Turbulence model: In (2), μ_{eff} is the effective viscosity coefficient, which equals the molecular viscosity coefficient, μ, plus the turbulent eddy viscosity coefficient, μ_t:

$$\mu_{eff} = \mu+\mu_t \tag{4}$$

The turbulent viscosity, μ_t, is modeled as the product of a turbulent velocity scale, V_t and a turbulent

length scale, ℓ_t, as proposed by Kolmogorov. Introducing a proportionality constant gives

$$\mu_t = \rho C_\mu \ell_t V_t \quad (5)$$

Both equation models take the velocity scale, V_t, to be the square root of the turbulent kinetic energy:

$$V_t = \sqrt{k} \quad (6)$$

The turbulent kinetic energy, k, is determined from the solution of a semi-empirical transport equation. In the standard k-ε two-equation model it is assumed that the length scale is a dissipation length scale and when the turbulent dissipation scales are isotropic, Kolmogorov determined that

$$\varepsilon = \frac{k^{3/2}}{\ell_t} \quad (7)$$

where ε is the turbulent dissipation rate.

Therefore, the turbulence viscosity, μ_t, can be derived from (5),(6) and (7) to link to the turbulence kinetic energy and dissipation via the relation

$$\mu_t = C_\mu \rho \frac{k^2}{\varepsilon} \quad (8)$$

where C_μ is a constant. Its value is 0.09.

The values of k, ε come directly from the differential transport equations for the turbulence kinetic energy and turbulence dissipation rate:

$$\nabla.(\rho U k) - \nabla.(\Gamma_k \nabla k) = p_k - \rho\varepsilon \quad (9)$$

And

$$\nabla\cdot(\rho U \varepsilon) - \nabla\cdot(\Gamma_\varepsilon \nabla\varepsilon) = \frac{\varepsilon}{k}(C_{\varepsilon 1} p_k - C_{\varepsilon 2}\rho\varepsilon) \quad (10)$$

where the diffusion coefficients are given by

$$\Gamma_k = \mu + \frac{\mu_t}{\sigma_k}$$

$$\Gamma_\varepsilon = \mu + \frac{\mu_t}{\sigma_\varepsilon}$$

and $\sigma_\varepsilon = 1.3$ are constants.

The p_k in (9) and (10) is the turbulent kinetic energy production term, which for incompressible flow is

$$p_k = \mu_t \nabla U \cdot \left(\nabla U + \nabla U^T\right) - \frac{2}{3}\nabla\cdot U(\mu_t \nabla\cdot U + \rho k) \quad (11)$$

Equations (1), (2), (9) and (10) form a closed set of nonlinear partial differential equations governing the fluid motion.

Boundary conditions: At the inlet, a steady, uniform, axial velocity distribution is imposed. This velocity specifies the flow rate. At the outlet, the fully developed condition is maintained. For this condition the length of outlet pipe is obtained from the (12).

$$L \cong 4.4 D_{H,out} Re^{\frac{1}{6}} \quad (12)$$

Where L is the pipe length, $D_{H,out}$ (=65 mm) is outlet hydraulic diameter and Re is the Reynolds number.

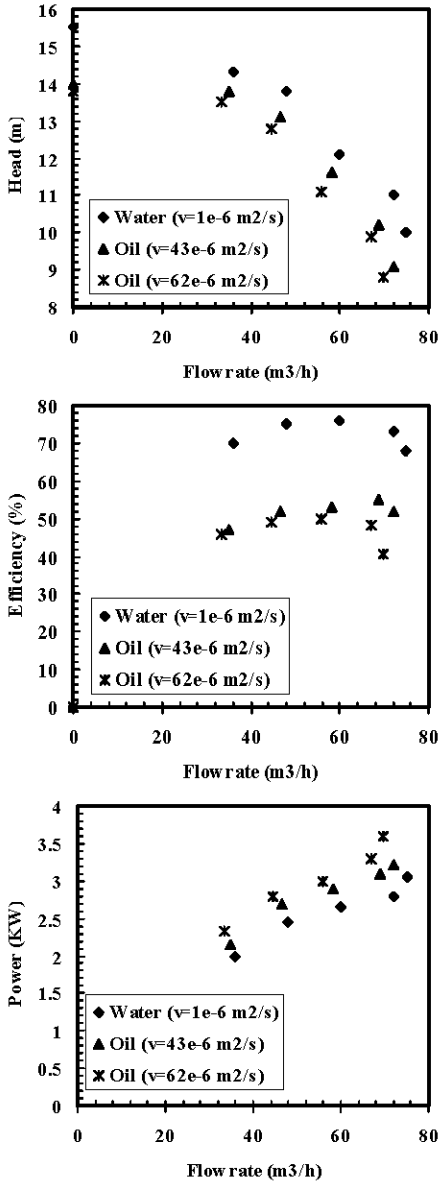

Fig. 7: The experimental effect of oil viscosities on the performance of centrifugal pump in comparison with water: (a) head, (b) power and (c) efficiency

Non slip boundary conditions have been imposed over the impeller blades and walls, the volute casing and the inlet pipe wall and the roughness of all walls is considered 100 μm.

The turbulence intensity at the inlet is totally depends on the upstream history of flow. Since the fluid in the suction tank is undisturbed, the turbulence intensity for all conditions is considered 1%.

In fully developed duct flows, turbulent length scale is restricted by the size of the duct. An approximate relationship between ℓ_t and the physical size of the duct is:

$$\ell_t = 0.07D_H \quad (14)$$

Using the above relation, the turbulence length scale at the inlet ($D_{H,in} = 80\,mm$) is estimated 5.6 mm.

Numerical solution control: The iterations number has been adjusted to reduce the residual below an acceptable value in each step. The numerical results dependence on the grid size has been tested with a lower number of cells. The overall performance of the pump is the same even with less than a half the cells. Flow main characteristics do not change.

RESULTS AND DISCUSSION

Figure 7 shows the centrifugal pump performances while the pump handles water with kinematic viscosity and viscous oils with viscosities 43×10^{-6} and 62×10^{-6} m^2/s at rotating speed 1450 rev/min at 20°C. The Best Efficiency Point (BEP) located at Q=60, 58.2 and 55.8 m^3/hr, corresponding to the best efficiencies are 76, 53 and 50% respectively. The head and efficiency for the pump handling oils are lower than those for handling water as shown in Fig. 7a and b, but the power-input for handling oil is higher than that for handling water as shown in Fig. 7c.

The pump efficiency dropping while pumping the oil results from the fact that the disc friction losses over the out-sides of the impeller shroud and hub as well as hydraulic losses in flow channel of pump are increasing rapidly. In order to verify this fact, additional experimntal work have been done for testing the impeller disc friction loss as the oils viscosities increase. Suppose that the disc loss does not depend on pump work condition, so the test data in shut-off condition can be used to estimate the disc loss. The losses in pump involve two parts, one is the disc friction loss and the other is the vortex loss due to the interaction between impeller and volute in the shut-off condition. The disc friction loss can be evaluated by using Pfleiderer's (1955) famous formula, pumping water. The vortex loss for pumping water will be estimated through subtracting the disc friction loss from the power-input in shut-off condition. This vortex loss is assumed to maintain the same value while pumping the oils, therefore the disc friction losses will be estimated through subtracting the vortex loss from the power-input in shut-off condition for higher kinematic viscosity fluid. From the additional experimental data, the disc friction losses relate to the kinematic viscosity of the working fluids follows:

$$\frac{P_{ds}}{P} = 0.098\times1.0109^{v} \quad (15)$$

Where P_{ds}, P and v represent the disc friction loss, power input and the kinematic viscosity, respectively. This equation is a regression equation only for the available data in which the kinematic viscosity of fluid is $<63\times10^{-6}$ m^2/s. meanwhile, the hydraulic loss for pumping oil 43×10^{-6} and 62×10^{-6} m^2/s increases to 39 and 41% from 26% for handling the water.

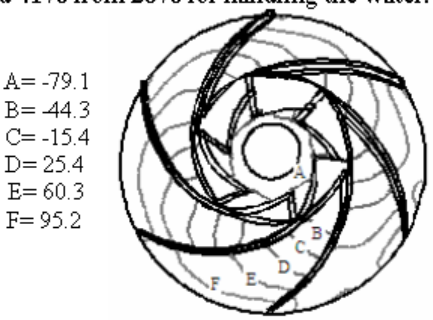

Fig. 8: The static pressure (KPa) contours in impeller when handling the water ($v=1\times10^{-6}$ m^2/s)

Fig. 9: The static pressure (KPa) contours in impeller when handling the oil ($v=43\times10^{-6}$ m^2/s)

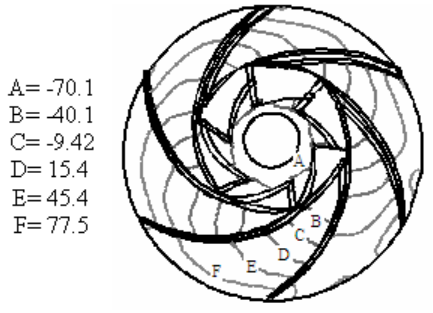

Fig. 10: the static pressure (KPa) contours in impeller when handling the oil ($v=62\times10^{-6}$ m^2/s)

Figure 8-10 show the static pressure contours in BEP (Best Efficiency Point) for various viscous fluids in impeller with 27.5° blade outlet angle. The numerical head of pump handling the water, oil 43 and 62 is 11.8,

10.9 and 10.5, respectively in BEP. The error of numerical and experiment head is less than 3%.

For finding the accuracy of 3D model, the numerical simulations were done for different flow rates for each fluid for impeller with outlet angle 27.5°. after finding the agreement of numerical and experimental resuts, simulations were used for various blade outlet angles. Figure 11 and 12 show the comparison between numerical and experimental results for various blade outlet angles. Figure 13 and 14 show the relative velocity profiles of oils between blade

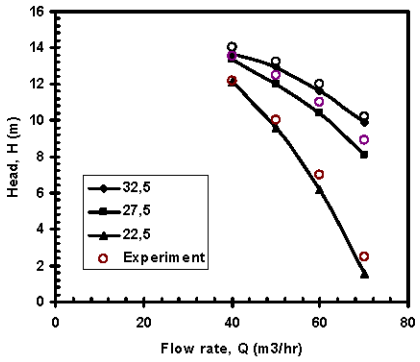

Fig. 11: Influence of different blade outlet angles on performance of centrifugal pump when handling the oil (ν=43×10^{-6} m^2/s)

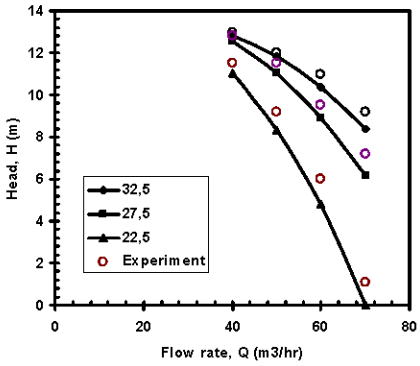

Fig. 12: Influence of different blade outlet angles on performance of centrifugal pump when handling the oil (ν=62×10^{-6} m^2/s)

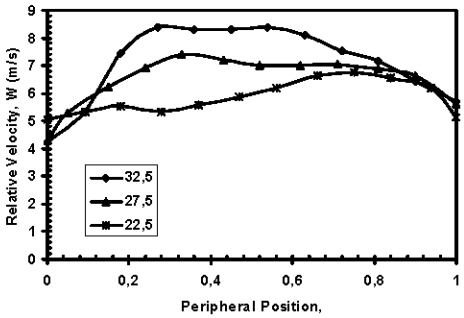

Fig. 13: The Comparison of relative velocity at the outlet of impeller when handling the oil (ν=43×10^{-6} m^2/s)

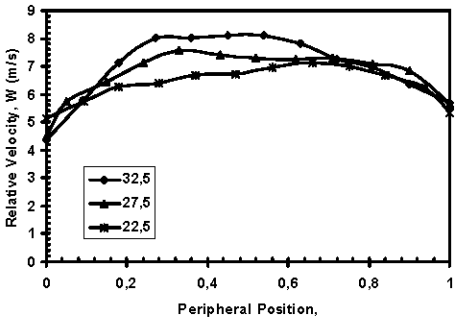

Fig. 14: The Comparison of relative velocity at the outlet of impeller when handling the oil (ν=62×10^{-6} m^2/s)

to blade in middle span z=6.5 mm stream surface at the exit of impeller in BEP, where θ, θ_o and W represent peripheral angle, center angle between bade pressure and suction sides at same radius, as well as relative velocity of the fluids, respectively.

Due to these profiles the velocity near the SS is almost equal to those near PS, the variation trend of the profile is not similar to those predicted by the potential flow theory.

CONCLUSION

With regards to the test pump and numerical simulation in the present study the following conclusions can be drawn:

* The reason why a centrifugal pump performance goes down when the pump handles high viscosity working fluids is that high viscosity results in a rapid increase in the disc friction losses over outsides of the impeller shroud and hub as well as in hydraulic losses in flow channels of pump.
* The three dimensional view of the pressure over the shroud, blades and part of the volute for the nominal flow point shows that pressure in the hub side is higher than in shroud, due to the transition of flow from the axial to the radial direction. Also, the flow impact over the tongue varies from the center -where the flow comes directly from the impeller- to the sides.
* Pressure distribution over the suction and pressure side of the blades when flow rate is the nominal one is clearly appreciated.
* When the blade outlet angle increases, the width of wake at the outlet of impeller decreases, this phenomenon causes the improvement of centrifugal pump performance when handling viscous fluids.
*. The numerical simulations and agreement of experimental tests results show that a wake separated is found near the suction side and a jet does not exist near blade pressure side, so that the

well known jet/ wake flow model is not found in the impeller when handling viscous fluids.

Nomenclature

BEP: Best efficiency point
D_H: Hydraulic diameter
H: Head
I: Turbulent intensity
k: Turbulent kinetic energy
L: Pipe Length
OL: Over Loading
P: Pressure, Power-input
P_{ds}: Disk friction loss
p_k: Turbulent kinetic energy production
PL: Part Loading
PS: Pressure side of blade
Q: Flow rate
Re: Reynolds number
$\vec{r}$: Location vector
SS: Suction side of blade
S_M: Source term
U: Velocity
u_{avg}: Turbulence average velocity
u_t: Velocity tangent to the wall
u': Velocity fluctuation
V_t: Turbulent velocity scale
W: Relative velocity
y: Distance from the wall

Greek symbols

δ: Identity matrix
Δ: Difference
ε: Dissipation
η: Efficiency
θ: Peripheral angle
θ_o: Center angle between blade pressure and suction sides
ℓ_t: Turbulent length scale
κ: Von Karman constant
μ: Molecular viscosity coefficient
μ_{eff}: Effective viscosity coefficient
μ_t: Turbulent eddy viscosity coefficient
ν: Kinematics Viscosity
ρ: Density
τ_w: Turbulent wall shear stress
$\vec{\Omega}$: Rotation speed
∇: Gradient
$\otimes$: Vector cross- product

REFERENCES

1. Stepanoff, A.J., 1940. Pumping viscous oils with centrifugal pumps. Oil and Gas J., No. 4.
2. Telow, N., 1942. A survey of modern centrifugal pump practice for oilfield and oil refinery services. The Institution of Mechanical Engineering, No. 121.
3. Ippen, A.T., 1946. The influence of viscosity on centrifugal pump performance. Trans. ASME, pp: 823.
4. Itaya, S. and T. Nishikawa, 1960. Studies on the volute pumps handling viscous fluids. Bull. JSME, 26: 202.
5. Stoffel, B., 1980. Tests on centrifugal pumps for handling viscous liquids. Institute of Chemical Engineers, Paper No. 3.
6. Li, W.G., 1996. LDV measurements and calculations of internal flows in the volute and impellers of a centrifugal oil pump. Fluids Machinery, 22: 2.
7. Li, W.G. and Z.M. Hu, 1997. An experimental study on performance of centrifugal oil pump. Fluids Machinery, 25: 3-7.
8. Denton, D., 1986. The use of a distribution body force to simulate viscous effects in 3D flow calculation. ASME J. Turbo Machinery, 86: GT-144.
9. Miner, S.M., 1992. Two dimensional flow analysis of a laboratory centrifugal pump. ASME J. Turbo Machinery, Vol. 114.
10. Miner, S.M., 1992. Turbulence measurement in a centrifugal pump with a synchronously orbiting impeller. ASME J. Turbo Machinery, Vol. 114.
11. Croba, D. and J.L. Kueny, 1996. Numerical calculation of 2D, unsteady flow in centrifugal pumps: Impeller and volute interaction. Intl. J. Numerical Methods in Fluids, 22: 467-481.
12. Denus, C.K. and E. Gode, 1999. A study in design and CFD analysis of a mixed-flow pump impeller. ASME-FEDSM-99-6858.
13. Blanco, E., 2000. Numerical flow simulation in a centrifugal pump with impeller-volute interaction. ASME-FEDSM200-11297.
14. Blanco, E., 2000. Numerical simulation of centrifugal pumps. ASME-FEDSM200-11162.
15. Varley, F.A., 1961. Effects of impeller design and surface goughness on performance of centrifugal pumps. Proc. Institution of Mechanical Engineers, 175: 955-989.
16. Li, W. and D. Xialing, 2000. Flow measurements in a centrifugal pump impeller when handling viscous oil. J. Mech. Engg., 36: 33-36.
17. Li, W., 2002. Influence of the number of impeller blades on the performance of centrifugal oil pumps. World Pumps, 410: 32-36.
18. Shojaee Fard, M.H. and M.B. Ehghaghi, 2002. Experimental and numerical study of centrifugal pump in the performance of viscous flow. Intl. J. Engg. Sci., 13: 35-52.